International Journal of Microwave and Wireless Technologies

cambridge.org/mrf

Decomposition of respiratory and cardiac phase fluctuations using dual-band distributed CW radar

Min Kim[1], Eugin Hyun[2], Youngseok Jin[2], Jieun Bae[2], Sangbin Cha[3], Jieun Lee[4] and Inoh Choi[4]

[1]Department of Maritime ICT and Mobility Research, Korea Institute of Ocean Science and Technology, Busan, South Korea; [2]Department of Future Automotive Technology Research, Daegu Gyeongbuk Institute of Science and Technology, Daegu, South Korea; [3]Department of Electronic Engineering, Pukyong National University, Busan, South Korea and [4]Department of Smart Mobility Engineering, Pukyong National University, Busan, South Korea

Research Paper

Cite this article: Kim M, Hyun E, Jin Y, Bae J, Cha S, Lee J, Choi I (2025) Decomposition of respiratory and cardiac phase fluctuations using dual-band distributed CW radar. *International Journal of Microwave and Wireless Technologies* **17**(9), 1506–1515. https://doi.org/10.1017/S1759078725102481

Received: 26 January 2025
Revised: 6 October 2025
Accepted: 17 October 2025

Keywords:
cardiac rate; dual-band distributed continuous wave radar; high-order harmonics; independent component analysis; respiratory rate

Corresponding author: Inoh Choi;
Email: inoh@pknu.ac.kr

Abstract

Respiratory and cardiac rates can be estimated by analyzing a spectrum of linearly mixed phase fluctuations in a radar echo of an individual. However, there are high-order harmonics caused by time-varying respiratory rate, and the interference effect of the respiratory rate and its harmonics makes it difficult to estimate the cardiac rate with relatively low energy in a spectrum. To solve this problem, we exploit the independent component analysis method with dual-band distributed continuous wave radar for effective decomposition of phase fluctuations corresponding to respiratory and cardiac rates. In simulations and experiments, the respiratory and cardiac rates were successfully estimated by the proposed decomposition method, compared with conventional methods.

Introduction

Vital sign (i.e., respiratory and cardiac rates) estimation of an individual using a radar sensor is important to applications of health care [1–5]. Respiratory and cardiac micro-motions at the human chest cause linearly mixed phase fluctuations in a radar echo, so the vital sign estimation process generally requires 1) decomposition of phase fluctuations corresponding to respiratory and cardiac rates; 2) spectral analysis of the decomposed phase fluctuations [6]. Especially, for decomposition of the phase fluctuations, either a low-pass filter or a high-pass filter is usually adopted [7], but when the cardiac rate is decreased heading to the respiratory rate, the decomposition using these filters may fail. In addition, when the respiratory rate is imperceptibly time-varying during observation time in the scale of seconds, it inevitably generates several harmonics of the respiratory rate in a spectrum [7]. Especially, when the 2nd and 3rd order harmonics coincide with the cardiac rate, it may fail in the cardiac rate estimation because of the interference between them.

An alternative is to utilize sophisticated decomposition techniques such as wavelet transform [8], empirical mode decomposition [9, 10], and variational mode decomposition [11–13]. These methods can decompose phase fluctuations into each component in different bands. In [14], the pruned exact linear time algorithm and the ensemble empirical mode decomposition have been proposed to suppress the interference signal and extract the vital signal. Moreover, the recursive least squares-based adaptive filter [15] was exploited to suppress several harmonics of the respiratory rate. However, when the cardiac rate is similar to the respiratory rate in a frequency domain, these methods may fail to decompose them. In addition, deep learning methods can be utilized to solve this problem, but it is difficult to obtain big radar data for humans in several situations.

In this article, we utilize the independent component analysis (ICA) algorithm [16–18] with a compact dual-band distributed continuous wave (CW) radar system for effective decomposition. Assume that two unknown parameters x (i.e., independent phase fluctuations caused by respiratory and cardiac micro-motions) are linearly mixed by the determined system, such as $\mathbf{A}x = b$, where $\mathbf{A}$ is the unknown mixing matrix with full rank and b is the measurements. Then, the full rank of $\mathbf{A}$ can be guaranteed by the use of different carrier frequencies and spatial diversity in the dual-band distributed CW radar system. Here, the ICA algorithm can be exploited to estimate the mixing matrix $\widehat{\mathbf{A}}$, thus two unknown parameters $\hat{x}$ can be calculated by $\hat{x} = \widehat{\mathbf{A}}^{-1}b$. By means of spectral analysis of $\hat{x}$, the respiratory and cardiac rates can be more robustly estimated due to the proposed decomposition process, unlike conventional methods. An earlier version of this paper was presented at EuMW 2024 and was published in its Proceedings [1].

© The Author(s), 2025. Published by Cambridge University Press in association with The European Microwave Association.

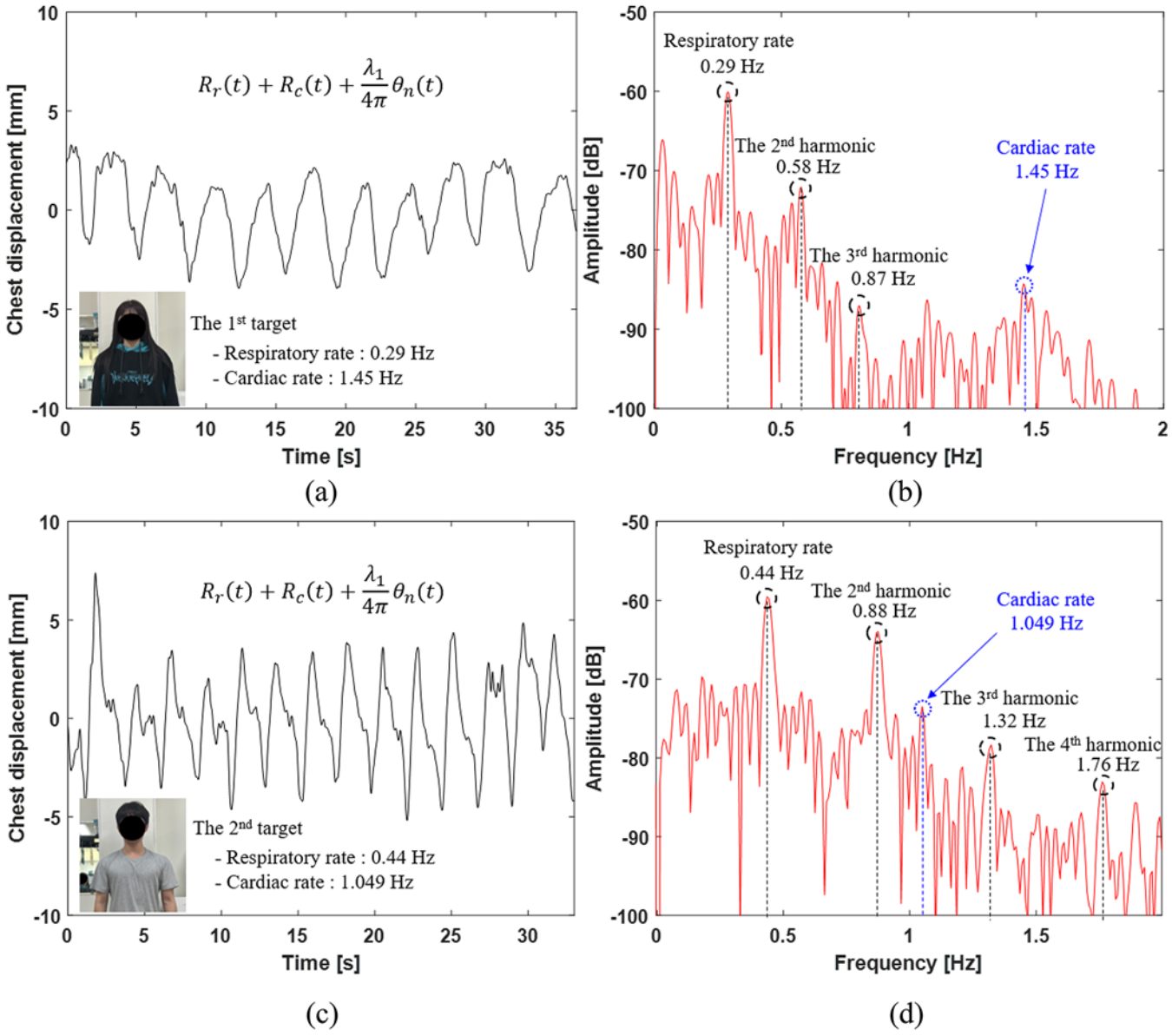


Figure 1. Example of measurements for two targets. (a) Chest displacement obtained by scaling of phase fluctuations and (b) its spectrum for the 1st target. (c) Chest displacement obtained by scaling of phase fluctuations and (d) its spectrum for the 2nd target.

The rest of this article is organized as follows. Signal model and discussion introduces signal model and discusses some difficulties in a vital sign estimation scheme. Proposed method describes the proposed method in detail. Results provides simulation and experimental results to verify the proposed method. Finally, Conclusion concludes this article.

Signal model and discussion

Signal model for vital sign estimation

We assume that a CW radar signal is returned from an ideal point scatterer (i.e., solution using the geometrical theory of diffraction [19] to evaluate the radiated field of a rigid body model) of the human chest engaged in the micro-motions with respiratory and cardiac rates [6, 7]. Then, the returned signal $s_r(t)$ at baseband can be defined as follows:

$$s_r(t) = I(t) + jQ(t) = \sqrt{P_r(t)}exp[j\theta(t)] + n(t) \quad (1)$$

where $I(t)$ is the real part of $s_r(t)$, $Q(t)$ is the imaginary part of $s_r(t)$, $\theta(t)$ is the phase modulated by the micro-motions, and the received power $P_r(t)$ is

$$P_r(t) = \frac{P_t G_t G_r \lambda^2 \sigma}{(4\pi)^2 \{R(t)\}^4} \quad (2)$$

where P_t is the transmitted power, G_t is the antenna gain of the transmitter, G_r is the antenna gain of the receiver, λ is the wavelength, σ is the radar cross section, and $R(t)$ is the radial distance between the CW radar and the point scatterer. In (1), $n(t)$ is the random white Gaussian thermal noise with the ensemble average power $E\{P_n\} = kTBW_{eff}$, where k is the Boltzmann constant, T is

https://doi.org/10.1017/S1759078725102481 Published online by Cambridge University Press

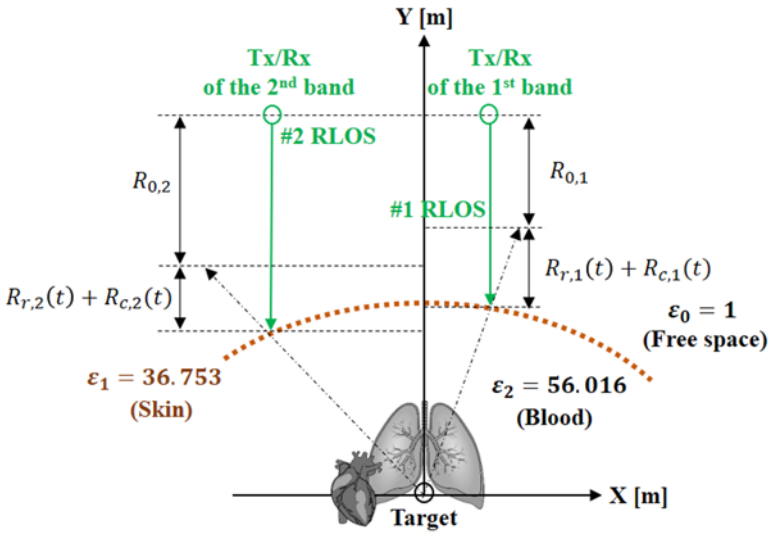


Figure 2. Geometry of vital-sign estimation with dual-band distributed CW radar system.

Table 1. Simulation parameters

Wavelength of the 1st band (λ_1)	0.06 m
Wavelength of the 2nd band (λ_2)	0.0517 m
Sampling rate	20 Hz
SNR	30 dB
Maximum radial distance of respiratory rate at the 1st band ($d_{r0,1}$)	0.004 m
Maximum radial distance of respiratory rate at the 2nd band ($d_{r0,2}$)	0.007 m
Respiratory rate (f_{r0})	0.33 Hz
Maximum radial distance of cardiac rate at the 1st band ($d_{c0,1}$)	0.0003 m
Maximum radial distance of cardiac rate at the 2nd band ($d_{c0,2}$)	0.0004 m
Cardiac rate (f_{c0})	1 Hz
Observation time	25 s
Initial radial distances at the 1st band ($R_{0,1}$)	0.2 m
Initial radial distances at the 2nd band ($R_{0,2}$)	0.5 m

the absolute temperature, and BW_{eff} is the effective bandwidth. In (1), $\theta(t)$ can be defined using the radial distance $R(t)$ in (2) as

$$\theta(t) = \frac{4\pi}{\lambda} R(t) = \frac{4\pi}{\lambda} \{R_0 + R_r(t) + R_c(t)\} \quad (3)$$

where R_0 is the initial radial distance, $R_r(t)$ is the radial distance caused by the chest's micro-motion with respiratory rate as

$$R_r(t) = d_{r0} cos\{2\pi f_r(t)\, t + \varphi_{r0}\} \quad (4)$$

where d_{r0} is the maximum radial distance caused by the respiratory motion, φ_{r0} is the initial phase offset, and

$$f_r(t) = f_{r0} \pm \Delta f_r(t) \quad (5)$$

is the time-varying respiration rate function. Here, f_{r0} is the respiration rate and $\Delta f_r(t)$ is the slight variation of the respiration rate, leading to high-order harmonics in the spectrum of (3) due to the nonlinear relation between the input and output in the fast Fourier transform process [7]. In (3), $R_c(t)$ is the range distance caused by the chest's micro-motion with cardiac rate as

$$R_c(t) = d_{c0} cos\{2\pi f_c(t)\, t + \varphi_{c0}\} \quad (6)$$

where d_{c0} is the maximum radial distance caused by the cardiac motion, φ_{c0} is the initial phase offset, and

$$f_c(t) = f_{c0} \pm \Delta f_c(t) \quad (7)$$

is the time-varying cardiac rate function. Here, f_{c0} is the cardiac rate and $\Delta f_c(t)$ is the slight variation in the cardiac rate.

Difficulties in cardiac rate estimation

For vital-sign estimation, the phase fluctuations can be approximately extracted by applying the arctangent demodulation [6] to (1) as

$$tan^{-1}\left(\frac{Q(t)}{I(t)}\right) \approx \frac{4\pi}{\lambda} \{R_0 + R_r(t) + R_c(t)\} + \theta_n(t) \quad (8)$$

where $\theta_n(t)$ is the phase term of the thermal noise $n(t)$ in (1). The fundamental frequencies, such as f_{r0} and f_{c0}, in the spectrum of (8) can be estimated as the respiratory and cardiac rates, respectively. However, existing methods [8–15] may fail to estimate the cardiac rate f_{c0} due to the problem: phase fluctuations caused by the time-varying respiratory rate in (5) make high-order harmonics, and these harmonics interfere in estimating the cardiac rate in the spectrum.

To demonstrate this problem intuitively, we used the single-band Doppler radar [20] with a carrier frequency of 5.85 GHz, observation time 35 s, and sampling frequency 1 kHz. Measurements for two targets were independently obtained from an individual lying on the ground. Their chest displacements were obtained by scaling of phase fluctuations for measurements, and their spectrum could be calculated by fast Fourier transform (FFT) and squared (see Fig. 1). In the case of the 2nd target, high-order harmonics of the relatively high respiratory rate existed in the spectrum, so the cardiac rate estimation may be interrupted by them in similar bands, unlike the case of the 1st target. Moreover, if the energy of the cardiac rate in the spectrum is similar to that

https://doi.org/10.1017/S1759078725102481 Published online by Cambridge University Press

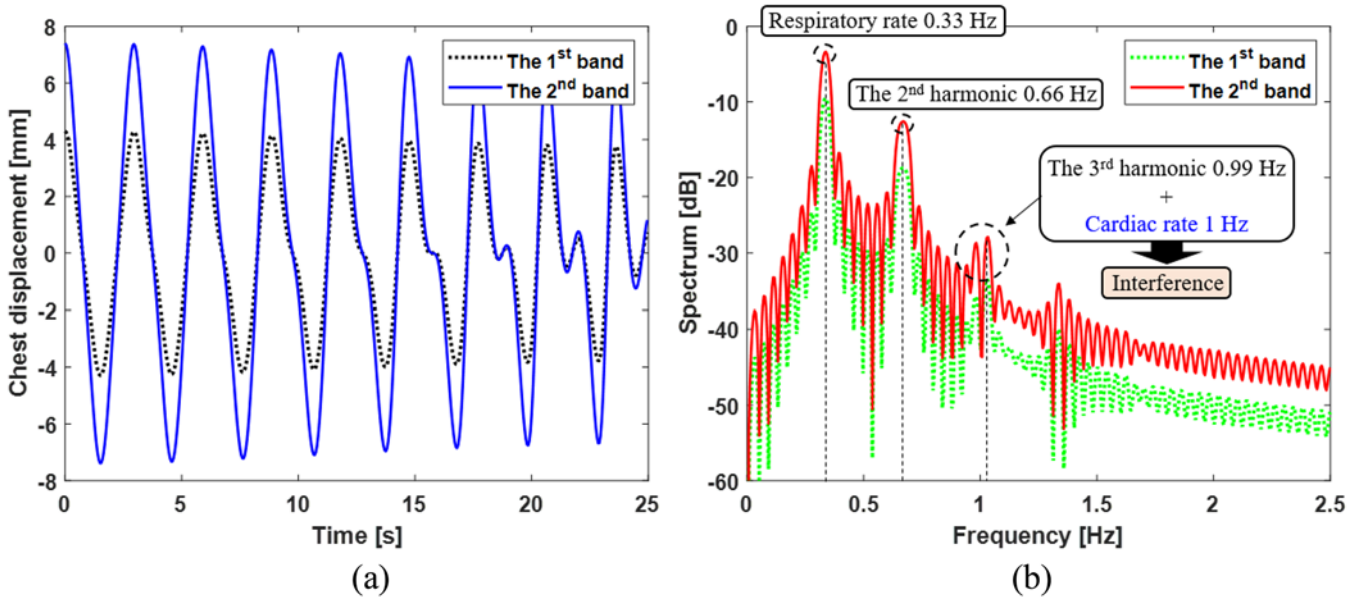


Figure 3. Example of (a) chest displacements and (b) their spectra for point scatterer model of the human chest with micro-motions of respiratory and cardiac rates in a dual-band distributed CW radar system.

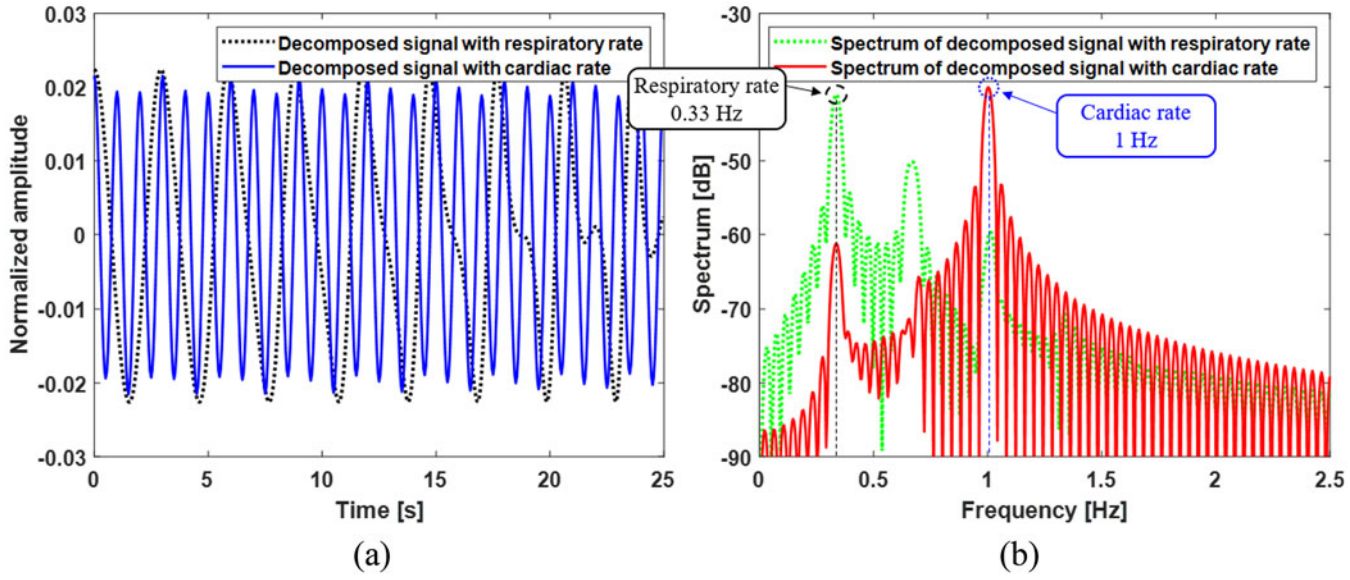


Figure 4. Simulation results to investigate the decomposition accuracy of the proposed method. (a) Decomposed signals and (b) their spectrums.

of the 3rd order harmonic, the cardiac rate may be undetectable despite the use of several existing methods [8–15]. Thus, it requires devising a new decomposition for robust cardiac rate estimation.

Proposed method

We assume that a dual-band distributed CW radar system is composed of two spatially-separated Txes and Rxes (i.e., two different radar line-of-sight), and the target consists of skin and blood with permittivity of $\varepsilon_1 = 36.753$ and $\varepsilon_2 = 56.016$, respectively [2] (see Fig. 2). Here, the kth (i.e., $k = 1, 2$) band Rx's echo signal reflected from an individual with vital signs is written by using (1) as

$$s_{r,k}(t) = I_k(t) + jQ_k(t) = \sqrt{P_{r,k}(t)}exp\left[j\theta_k(t)\right] + n_k(t) \quad (9)$$

And its phase fluctuations $b_k(t)$ can be extracted by the arctangent demodulation [15] as

$$b_k(t) = tan^{-1}\left(\frac{Q_k(t)}{I_k(t)}\right) \approx \frac{4\pi}{\lambda_k}\left\{R_{0,k} + R_{r,k}(t) + R_{c,k}(t)\right\} + \theta_{n,k}(t). \quad (10)$$

where

$$R_{r,k}(t) = d_{r0,k}cos\left\{2\pi f_r(t)\,t + \varphi_{r0}\right\} \quad (11)$$

$$R_{c,k}(t) = d_{c0,k}cos\left\{2\pi f_c(t)\,t + \varphi_{c0}\right\}. \quad (12)$$

Next, we derive the relationship between $\underline{\mathbf{b}}(t) = [b_1(t), b_2(t)]$ in (10) and $R_{r,k}(t)$ in (11) and $R_{c,k}(t)$ in (12) as a linear combination of samples:

https://doi.org/10.1017/S1759078725102481 Published online by Cambridge University Press

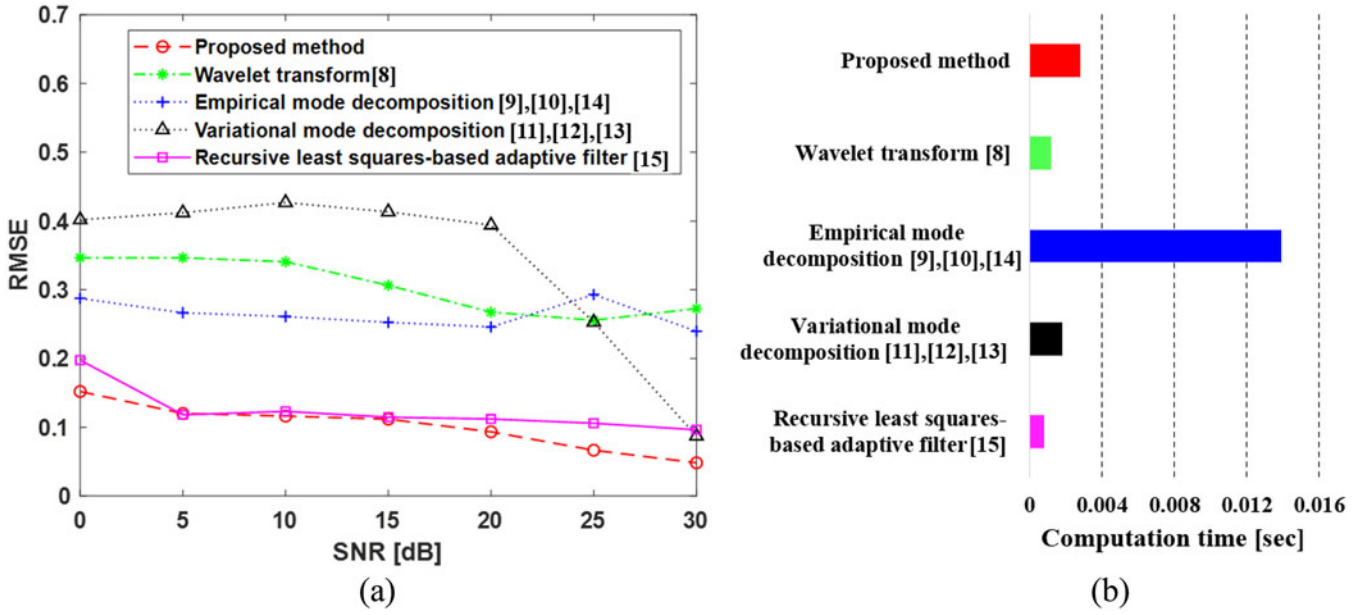


Figure 5. Quantitative evaluation of cardiac rate estimation for representative conventional methods [8–15] and proposed method in the special case of Figure 3. (a) RMSE versus SNRs. (b) Computation time.

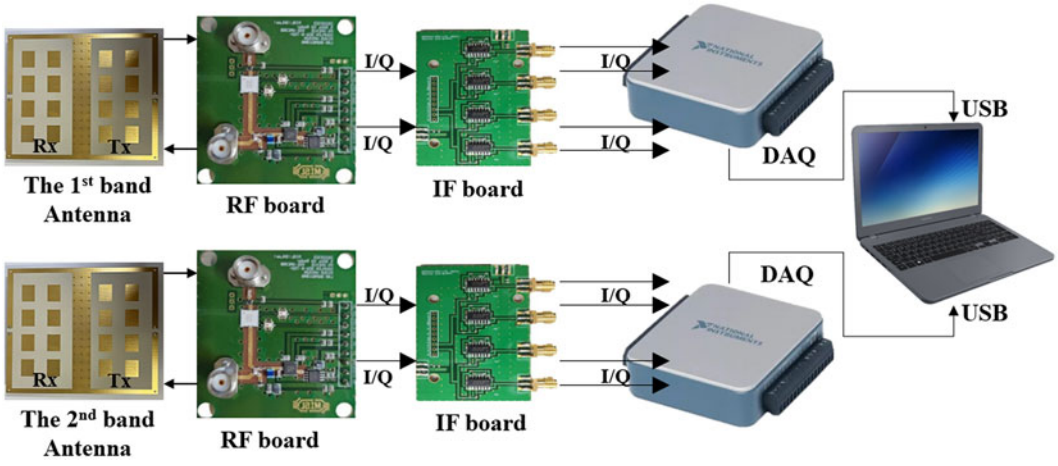


Figure 6. Configuration of dual-band distributed CW radar system [20] for proposed method.

$$\begin{aligned}\underline{\mathbf{b}}(t) &= \begin{bmatrix} \frac{4\pi}{\lambda_1} d_{r0,1} & \frac{4\pi}{\lambda_1} d_{c0,1} \\ \frac{4\pi}{\lambda_2} d_{r02} & \frac{4\pi}{\lambda_2} d_{c0,2} \end{bmatrix} \begin{bmatrix} cos\{2\pi f_r(t)\, t + \varphi_{r0}\} \\ cos\{2\pi f_c(t)\, t + \varphi_{c0}\} \end{bmatrix} \\ &\quad + \begin{bmatrix} \frac{4\pi}{\lambda_1} R_{0,1} \\ \frac{4\pi}{\lambda_2} R_{0,2} \end{bmatrix} + \begin{bmatrix} \theta_{n,1}(t) \\ \theta_{n,2}(t) \end{bmatrix} \\ &= \mathbf{A} \cdot \underline{\mathbf{x}}(t) + \underline{\mathbf{R}}_0(t) + \underline{\boldsymbol{\theta}}_n(t) \end{aligned} \tag{13}$$

In (13), two unknown signals $\underline{\mathbf{x}}(t)$ (i.e., $cos\{2\pi f_r(t)t + \varphi_{r0}\}$ and $cos\{2\pi f_c(t)\, t + \varphi_{c0}\}$ are linearly mixed by 2×2 mixing matrix $\mathbf{A}$, $\underline{\mathbf{R}}_0(t)$ is the phase offset caused by the initial radial distances, and $\underline{\boldsymbol{\theta}}_n(t)$ is the phase term of the thermal noise at each band. Even if the $\underline{\mathbf{R}}_0(t)$ in (13) is unknown constants, it can be removed by using the average values of the $\underline{\mathbf{b}}(t)$ (i.e., centering process [18]) as

$$\hat{\underline{\mathbf{b}}}(t) = \begin{bmatrix} b_1(t) \\ b_2(t) \end{bmatrix} - \begin{bmatrix} E\{b_1(t)\} \\ E\{b_2(t)\} \end{bmatrix} \approx \mathbf{A} \cdot \underline{\mathbf{x}}(t) + \underline{\boldsymbol{\theta}}_n(t). \tag{14}$$

Note that the unknown mixing matrix $\mathbf{A}$ can be full rank (i.e., rank($\mathbf{A}$) = 2) with different wavelength (i.e., λ_1 and λ_2) caused by carrier frequency diversity and different maximum radial distances (i.e., $d_{r0,1}$, $d_{c0,1}$, $d_{r0,2}$, and $d_{c0,2}$) caused by spatial diversity, and it can be achieved by using dual-band distributed CW radar system. To estimate the $\mathbf{A}$ in (14), we exploited the complex-valued FastICA algorithm in [18].

We define that the unknown mixing matrix $\mathbf{A}$ is composed of the matrices $\mathbf{V}$ and $\mathbf{W}$ (i.e., $\mathbf{A} = \mathbf{V}{\cdot}\mathbf{W}$). This algorithm is conducted in two steps: 1) a whitening process to estimate the matrix $\mathbf{V}$, and 2) estimation of the matrix $\mathbf{W}$ by maximization of non-Gaussianity. To accomplish the whitening process, the covariance of $\hat{\mathbf{b}}(t)$ is eigendecomposed as

https://doi.org/10.1017/S1759078725102481 Published online by Cambridge University Press

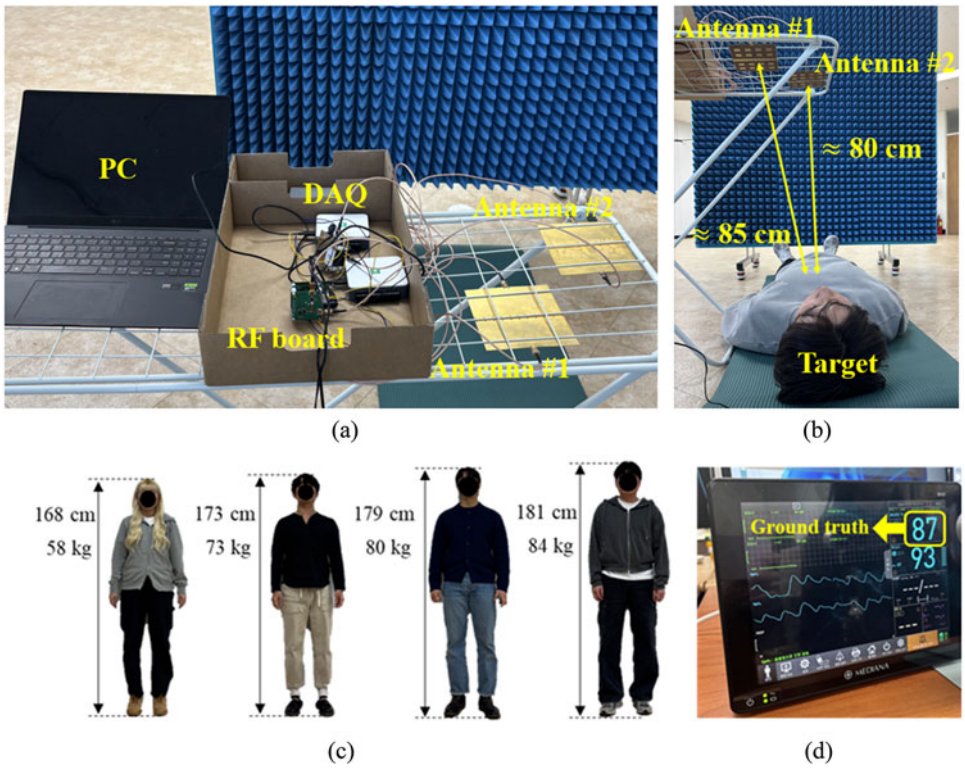


Figure 7. Measurements setup with (a) dual-band distributed CW radar system [20], (b) a target lying on the ground, (c) 4 targets, and (d) assessment tool to obtain the ground truth of cardiac rate.

$$\mathbf{C} = E\left\{\underline{\hat{\mathbf{b}}}(t)\,\underline{\hat{\mathbf{b}}}^{H}(t)\right\} = \mathbf{U}\cdot\boldsymbol{\Lambda}\cdot\mathbf{U}^{H} \tag{15}$$

Where $\boldsymbol{\Lambda}$ is the 2×2 diagonal matrix whose diagonal components are the two dominant eigenvalues that correspond to respiratory and cardiac rates, and $\mathbf{U}$ is the 2×2 orthonormal matrix that spans the respiratory and cardiac subspaces of $\mathbf{C}$. From (15), the whitening matrix can be estimated as

$$\widehat{\mathbf{V}} = \boldsymbol{\Lambda}^{-(1/2)}\cdot\boldsymbol{U}^{H}. \tag{16}$$

Next, to obtain the 2×1 vector $\hat{\mathbf{u}}(t)$ consisting of the uncorrelated signals, we apply the $\widehat{\mathbf{V}}$ to $\hat{\mathbf{b}}(t)$ in (14) as follows:

$$\begin{aligned}\underline{\hat{\mathbf{u}}}(t) = \widehat{\mathbf{V}}^{-1}\cdot\underline{\hat{\mathbf{b}}}(t) &= \widehat{\mathbf{V}}^{-1}\cdot\mathbf{A}\cdot\underline{\mathbf{x}}(t) + \widehat{\mathbf{V}}^{-1}\cdot\underline{\boldsymbol{\theta}}_{n}(t)\\ &= \mathbf{W}\cdot\underline{\mathbf{x}}(t) + \widehat{\mathbf{V}}^{-1}\cdot\underline{\boldsymbol{\theta}}_{n}(t)\end{aligned} \tag{17}$$

To estimate the $\mathbf{x}(t)$ in (17), we should find the 2×2 unitary matrix $\mathbf{W}$ to maximize the non-Gaussianity of the $\hat{\mathbf{u}}(t)$. Here, the approximated negentropy $E\left\{\log\left(1+\left|\underline{\boldsymbol{w}}_{k}^{H}\cdot\underline{\hat{\mathbf{u}}}(t)\right|^{2}\right)\right\}$ can be utilized as a cost function for iterative optimization to estimate the kth 2×1 column vector $\underline{\boldsymbol{w}}_{k}^{H}$ of the $\mathbf{W}$ [18]. Finally, we can estimate the two unknown independent phase fluctuations $\underline{\hat{\mathbf{x}}}(t)$ using the $\widehat{\mathbf{W}}$ as

$$\underline{\hat{\mathbf{x}}}(t) = \widehat{\mathbf{W}}^{-1}\cdot\underline{\hat{\mathbf{u}}}(t) = \underline{\mathbf{x}}(t) + \widehat{\mathbf{W}}^{-1}\cdot\widehat{\mathbf{V}}^{-1}\cdot\underline{\boldsymbol{\theta}}_{n}(t). \tag{18}$$

After the proposed decomposition, the respiratory and cardiac rates (i.e., f_{r0} and f_{c0}) can be independently obtained by analyzing the spectrum of the $\underline{\hat{\mathbf{x}}}(t)$. Then, the decomposed signal (i.e., $\hat{x}_2(t) \approx cos\{2\pi f_c(t)\,t+\varphi_{c0}\}$) with cardiac rate may be imperfectly separated because of residual errors in estimated $\widehat{\mathbf{W}}$. Nevertheless, the respiratory rate's harmonics in the $\hat{x}_2(t)$ can be simply removed by using the estimated respiratory rate from $\hat{x}_1(t) \approx cos\{2\pi f_r(t)\,t+\varphi_{r0}\}$.

Results

Simulation result using point scatterer model

To verify the effectiveness of the proposed method to decompose the chest displacements (i.e., scaled phase fluctuations) caused by the respiratory and cardiac motions, we used an ideal point scatterer model [19] of the human chest with micro-motions of respiratory and cardiac rates for the signal-to-noise ratio (SNR) 30 dB in a dual-band distributed CW radar system (see Table 1).

Chest displacements (Fig. 3a) and their spectra (Fig. 3b) at two different bands (i.e., 5 and 5.8 GHz) were obtained by a centering process [18] like (14) to remove the offsets caused by $R_{0,1} = 0.2$ m and $R_{0,2} = 0.5$ m, an FFT process, and squaring. Here, the 3rd harmonic for the respiratory rate coincided with the cardiac rate at 0.99–1 Hz, leading to difficulties in accurate cardiac rate estimation. Because of the interference problem in this special case, the conventional methods [8–15] will fail in cardiac rate estimation.

In contrast, application of the proposed method that uses the 1st and 2nd band's chest displacements accurately decomposed two independent signals corresponding to respiratory and cardiac rates (Fig. 4a). Especially, the determinant of the 2×2 estimated mixing matrix was—0.254, so the rank of this matrix was close to 2, resulting in successful separation of the chest displacements for the cardiac rate despite the interference problem by the

https://doi.org/10.1017/S1759078725102481 Published online by Cambridge University Press

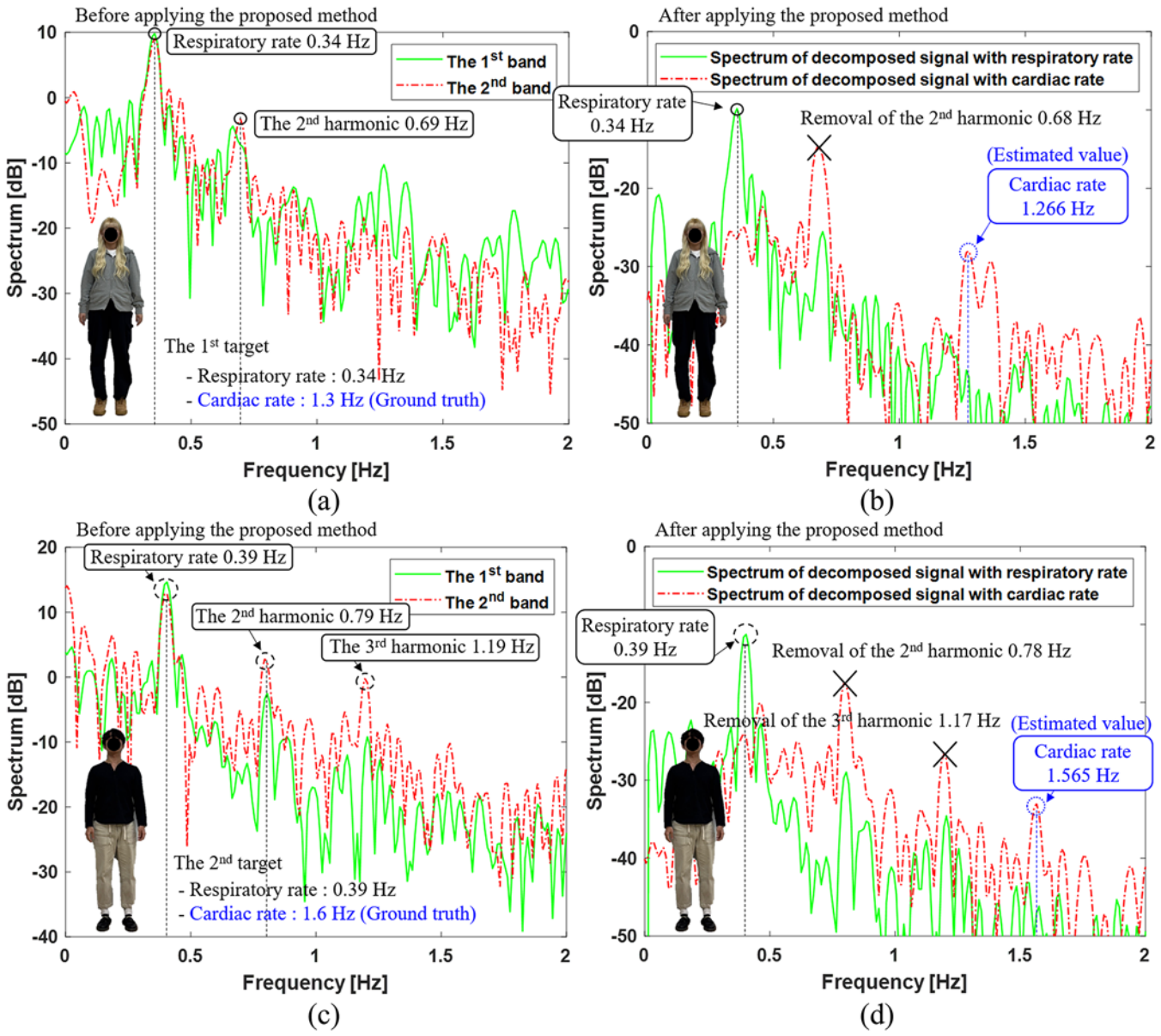


Figure 8. Example of spectra to verify the proposed method at observation time of 20 s. (a) Spectra of each band and (b) decomposed spectra for the 1st female target in Figure 7(c). (c) Spectra of each band and (d) decomposed spectra for the 2nd male target in Figure 7(c).

high-order harmonics of the respiratory rate. As a result, the respiratory and cardiac rates were successfully estimated by finding the fundamental frequencies in each spectrum of decomposed signals (Fig. 4b).

To verify the effect of the system noise on the cardiac rate estimation ability of the proposed method, we conducted 200 Monte Carlo simulations to compute the root mean squared error of the estimated cardiac rates for SNR = 0, 5, 10, 15, 20, 25, 30 dB. In Fig. 5(a), application of the proposed method estimated the cardiac rate accurately and reliably because of the decomposition between respiratory rate and cardiac rate, compared with the other methods [8–15]. In the case of the recursive least squares-based adaptive filter [15], reference signal for cardiac rate must be required to compute the filter coefficients, but it is difficult to obtain the reference signal in this special case. Therefore, Fig. 5(a) shows that our proposed method with dual-band distributed CW radar system can achieve reliable cardiac rate estimation with effective decomposition, compared to representative conventional methods.

To verify the computational efficiency of the proposed method, we compared the computational complexity of our proposed method with that of conventional methods in [8–15]. For this verification, we used MATLAB R2022a on a computer running Windows 11 with an AMD Ryzen 7 processor. Using 500 data samples per single Monte Carlo simulation, the computational time of the proposed method was ~0.0028 s (see Fig. 5b). The speedup occurs because the proposed method uses the complex-valued FastICA algorithm [18] with fixed point and Newton methods, whereas the empirical mode decomposition requires interpolation process to find extrema, leading to computational burden.

Therefore, these simulation results demonstrate that chest displacements for the cardiac rate can be accurately decomposed by using the proposed method despite the interference effect of chest

https://doi.org/10.1017/S1759078725102481 Published online by Cambridge University Press

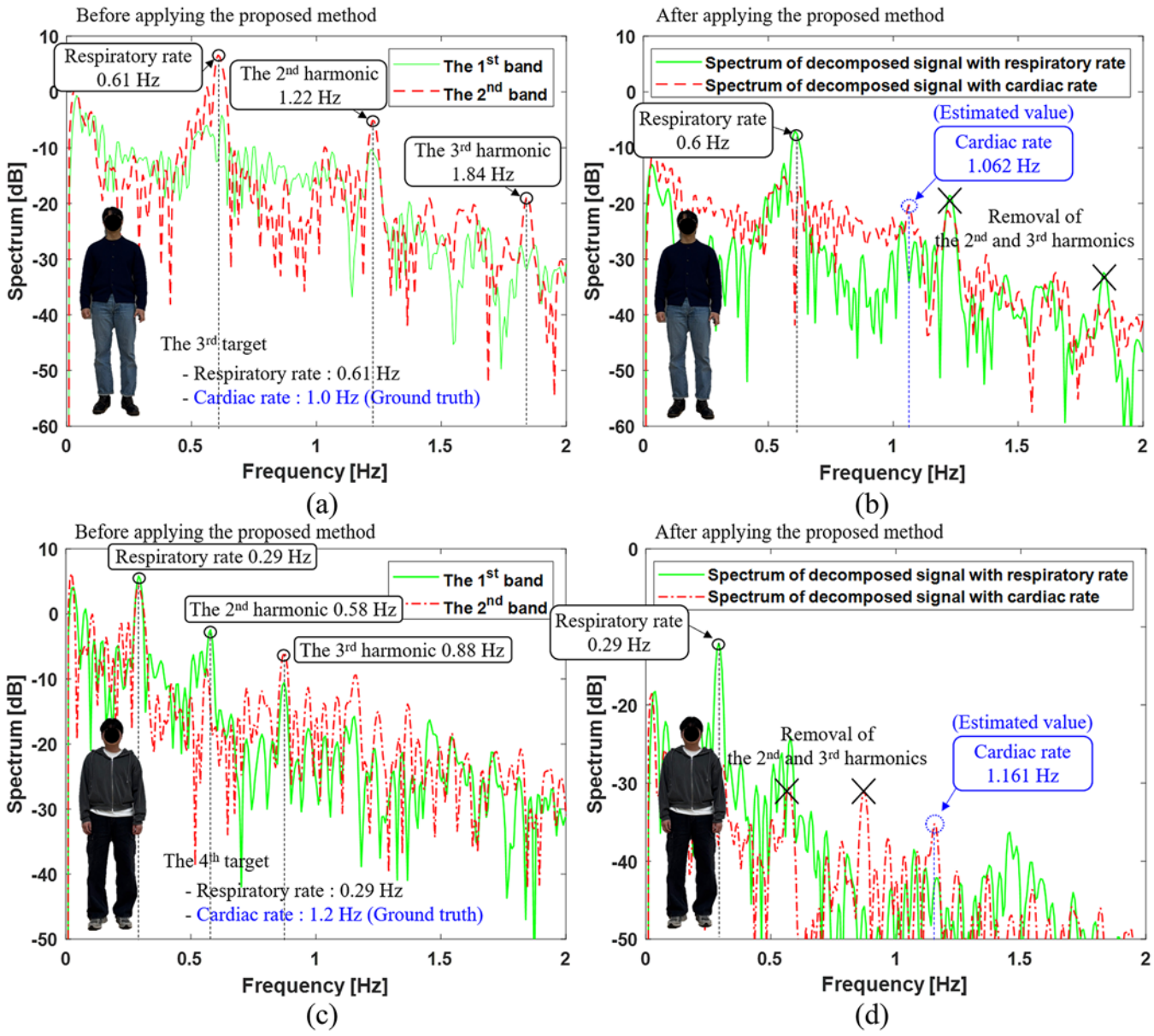


Figure 9. Example of spectra to verify the proposed method at observation time of 37 s. (a) Spectra of each band and (b) decomposed spectra for the 3rd male target in Figure 7(c). (c) Spectra of each band and (d) decomposed spectrums for the 4th male target in Figure 7(c).

displacements for the respiratory rate, so the cardiac rate can be accurately estimated by analyzing the spectrum of the decomposed signals.

Experimental result using dual-band distributed radar

Our dual-band distributed radar system with front-end CW Doppler radar modules [20] (see Fig. 6) was utilized to verify the decomposition ability of the proposed method, where the operational band was around 5.8 GHz due to high reflectivity for vital signs [21], and each band was selected as 5.7 and 5.85 GHz by using the voltage-controlled oscillator. We conducted experiments for an individual lying on the ground in an indoor environment (see Fig. 7a and b). For diversity of experimental conditions, measurements of the 1st and 2nd targets were obtained during observation time 20 sec, whereas those of the 3rd and 4th targets were obtained during observation time 37 sec (see Fig. 7c). The actual cardiac rate was measured by using a contact assessment tool (see Fig. 7d).

Chest displacements at the 1st and 2nd bands for the 1st and 2nd targets were decomposed by the proposed method as two independent signals, resulting in decomposed spectra corresponding to respiratory and cardiac rates (see Fig. 8). However, the decomposed spectrum with cardiac rate was imperfectly separated by residual errors in estimated $\widehat{\mathbf{W}}$ by the ICA algorithm [18] due to low energy of the cardiac rate (see Fig. 8b and d). In this case, the residual interference with the 2nd and 3rd harmonics of the respiratory rate could be removed by using the estimated respiratory rate from the spectrum of decomposed signal with respiratory rate, so the cardiac rates for the 1st and 2nd targets were estimated as 1.266 and 1.565 Hz.

In the case of the 3rd and 4th targets, chest displacements were obtained during 37 sec, leading to more high resolution (i.e., 0.027 Hz) in Doppler frequency domain (see Fig. 9). In addition,

https://doi.org/10.1017/S1759078725102481 Published online by Cambridge University Press

the ICA algorithm based on statistics can be more effectively implemented because of more samples. In Fig. 9(a), the 3rd target had the highest respiratory rate of 0.61 Hz, so it caused high harmonics (e.g., 1.22 and 1.84 Hz), unlike the 4th target in Fig. 9(c). Nevertheless, the energy of the respiratory rate in the decomposed signal with cardiac rate could be suppressed by the proposed method (see Fig. 9b). These experimental results show that the application of the proposed method can decompose the independent signal with cardiac rate, even though there are high-order harmonics of the respiratory rate.

Conclusion

This paper uses the ICA algorithm rates with a dual-band distributed radar system for effective decomposition of respiratory and cardiac signals. In simulations and experiments, the cardiac rate of an individual was successfully estimated because of the proposed decomposition approach.

Acknowledgments. This work was supported by the National Research Foundation of Korea (NRF) grant funded by the Korea government (MSIT) (No. RS-2023-00219725, Regional Leading Research Center on Development of Multimodal Untact Sensing for Life-Logging). And it was also funded by the project titled "Development of Polar Region Communication Technology and Equipment for Internet of Extreme Things (IoET)," funded by the Ministry of Science and ICT (MSIT), Republic of Korea (No. RS-2021-KS211508).

Competing interests. The author(s) declare none.

References

1. **Choi I, Park S, Kim M, Cha S, Jin Y, Bae J and Hyun H** (2024) Decomposition of respiratory and cardiac rates using dual band distributed radar. In *Proceedings of the 21st European Radar Conference (EuRAD)*, 324–327.
2. **Schires E, Georgiou P and Lande TS** (2018) Vital sign monitoring through the back using an UWB impulse radar with body coupled antennas. *IEEE Transactions on Biomedical Circuits and Systems* **12**, 292–302. https://doi.org/10.1109/TBCAS.2018.2799322
3. **Zhang Y, Qi F, Lv H, Liang F and Wang J** (2019) Bioradar technology: Recent research and advancements. *IEEE Microwave Magazine* **20**, 58–73. https://doi.org/10.1109/MMM.2019.2915491
4. **Chen KM, Huang Y, Zhang J and Norman A** (2000) Microwave life-detection systems for searching human subjects under earthquake rubble or behind barrier. *IEEE Transactions on Biomedical Engineering* **47**, 105–114. https://doi.org/10.1109/10.817625
5. **Forouzanfar M,Mabrouk M, Rajan S, Bolic M, Dajani HR and Groza VZ** (2016) Event recognition for contactless activity monitoring using phase-modulated continuous wave radar. *IEEE Transactions on Biomedical Engineering* **64**, 479–491. https://doi.org/10.1109/TBME.2016.2566619
6. **Adib F, Mao H, Kabelac Z, Katabi D and Miller RC** (2015) Smart homes that monitor breathing and heart rate. In *Proceedings of the 33rd Annual ACM Conference on Human Factors in Computing Systems*, 837–846.
7. **Choi I, Kim M, Choi J, Park J, Park S and Kim K** (2021) Robust cardiac rate estimation of an individual. *IEEE Sensors Journal* **21**, 15053–15064. https://doi.org/10.1109/JSEN.2021.3074510
8. **He M, Nian Y and Liu B** (2015) Noncontact heart beat signal extraction based on wavelet transform. In *Proceedings of the 8th International Conference on Biomedical Engineering and Informatics. (BMEI)*, 14–16.
9. **Feng J and Pan S** (2010) Extraction algorithm of vital signals based on empirical mode decomposition. *Journal of South China University of Technology* **38**, 1–6.
10. **Wang Y, Yang Z, Han L, Li Y and Zhang C** (2023) Extraction of vital sign based on improved complete ensemble empirical mode decomposition with adaptive noise for UWB radar. *2023 IEEE 6th International Electrical and Energy Conference (CIEEC)*, 2829–2834.
11. **Ding C, Yan J, Zhang L, Zhao H, Hong H and Zhu X** (2017) Noncontact multiple targets vital sign detection based on VMD algorithm. In *Proceedings of the IEEE Radar Conference (RadarConference)*, 8–12.
12. **Xia ZL, Wang XH, Wei HB and Xu Y** (2021) Detection of vital signs based on variational mode decomposition using FMCW radar. *2021 International Conference on Microwave and Millimetre Wave Technology (ICMMT)*, 1–3.
13. **Qu L, Liu C, Yang T and Sun Y** (2023) Vital sign detection of FMCW radar based on improved adaptive parameter variational mode decomposition. *IEEE Sensors Journal* **23**, 25048–25060. https://doi.org/10.1109/JSEN.2023.3312513
14. **Liu Z, Kong Y, Zhang X, Wu J and Wei L** (2020) Vital sign extraction in the presence of radar mutual interference. *IEEE Signal Processing Letters* **27**, 1745–1749. https://doi.org/10.1109/LSP.2020.3026942.
15. **Chen Y, Yuan J and Tang J** (2024) A high precision vital signs detection method based on millimetre wave radar. *Scientific Reports* **14**, 25535.
16. **Choi I, Kang K, Kim K and Park S** (2022) Use of ICA to separate micro-doppler signatures in ISAR images of aircraft that has fast-rotating parts. *IEEE Transactions on Aerospace and Electronic Systems* **58**, 234–246. https://doi.org/10.1109/TAES.2021.3098110
17. **Hyvarinen A, Karhunen J and Oja E**. (2001) *Independent Component Analysis*. Hoboken, NJ, USA: Wiley
18. **Bingham E and Hyvarinen A** (2000) A fast fixed-point algorithm for independent component analysis of complex valued signals. *International Journal of Neural Systems* **10**, 1–8. https://doi.org/10.1142/S0129065700000028
19. **Kammersgaard NPB, Kvist SH, Thaysen J and Jakobsen KB** (2019) Geometrical theory of diffraction formulation for on-body propagation. *IEEE Transactions on Antennas and Propagation* **67**, 1143–1152. https://doi.org/10.1109/TAP.2018.2882596
20. **Jin Y, Bae J, Choi I, Kim M, Park C and Hyun E** (2023) Detection method of human gait-rate and vital-sign using dual-baseband Doppler radar In *Apsar 2023*. Bali Island, Indonesia, pp. 1–4.
21. **Park J, Lee G, Lee I and Yang J** (2025) Heart rate extraction technique with mitigation of respiration harmonic for bio-radar sensors. *IEEE Sensors Journal* **25**, 929–939. https://doi.org/10.1109/JSEN.2024.3491753



Min Kim received the B.S. and M.S. degrees in electronic engineering from Pukyong National University, Busan, Korea, in 2015 and 2017, respectively. He received a Ph.D. degree in electronic engineering from Pohang University of Science and Technology, Pohang, South Korea, in 2022. Since 2023, he has been with the Maritime ICT & Mobility Research Department, Korea Institute of Ocean Science and Technology (KIOST), where he is currently a senior research scientist. His current research areas are radar target detection, human gait analysis, radar micro-Doppler signal processing, and sonar detection.



Eugin Hyun received the Ph.D., B.S., and M.S. degrees in electronic engineering from Yeungnam University, South Korea, in 2005, 2001, and 1999, respectively. He also received a B.S. in business administration from National Open University, South Korea, in 2008. Since 2005, he has been with Intelligence Sensor Signal-processing and System lab of the DGIST, South Korea, as an Executive Researcher. He also joined the Undergraduate Colleges, Yeungnam University as an Adjunct Professor from 2007 to 2018. He was invited as a Guest Researcher from Postech in 2018. His interests are radar system architecture design, Radar signal processing (detection, tracking, and classification) and machine learning of FMCW & CW radar, automotive applications for all-around and in-cabin, Smart city applications for surveillance and human monitoring, and multi-sensor fusion for commercial applications.

https://doi.org/10.1017/S1759078725102481 Published online by Cambridge University Press



Youngseok Jin received the B.S. and M.S. degrees in communication engineering from Daegu University, South Korea, in 2009 and 2012, respectively. Since 2012, he has been with Intelligence Sensor Signal-processing and System lab of the DGIST, South Korea, as a Researcher. His current interests include radar signal processing and implementation in FPGA/DSP.



Jieun Lee received the M.S. degree in electronic engineering from Keimyung University, South Korea, in 2020. Since 2021, she has been with Intelligence Sensor Signal-processing and System lab of the DGIST, South Korea, as a Researcher. Her interests are radar signal verification, radar test-bed implementation, and measurements.



Sangbin Cha received the B.S. and M.S. degrees in electronic engineering from Pukyong National University, Busan, South Korea, in 2017 and 2019, respectively, where he is currently pursuing the Ph.D. degree in electronic engineering. His research interests include the areas of radar target imaging and recognition, radar signal processing, target motion compensation, pattern recognition using artificial intelligence, radar cross-section prediction, and electromagnetic analysis of the wind farm.



Jieun Lee received the B.S. in mechanical system engineering from Pukyong National University, Busan, South Korea, in 2024, where she is currently pursuing the M.S. degree in smart mobility engineering. Her interests are radar detection of blood oxygen saturation, radar classification of gaiting humans.



Inoh Choi received the B.S. and M.S. degrees in electronic engineering from Pukyong National University (PKNU), Republic of Korea, in 2012 and 2014, respectively. He received the Ph.D. degree in electronic engineering from Pohang University of Science and Technology, Republic of Korea, in 2020. From 2019 to 2021, he was a senior researcher with the Agency for Defense Development, Republic of Korea. From 2021 to 2024, he was a faculty member (Tenure track) with the Division of Electronics and Electrical Information Communication Engineering, National Korea Maritime & Ocean University, Republic of Korea. Since 2024, he has been with the Department of Smart Mobility Engineering of the PKNU, where he is currently an Assistant Professor (Tenure track). Since September 2025, he has been a Vice Dean of College of Information Technology and Convergence at the PKNU. His current research area of interest includes radar target detection, dual-band radar resource management, micro-Doppler signature analysis, ballistic target discrimination, vital sign detection, estimation of oxygen saturation, automotive target recognition, and calibration of polarimetric synthetic aperture radar.

https://doi.org/10.1017/S1759078725102481 Published online by Cambridge University Press